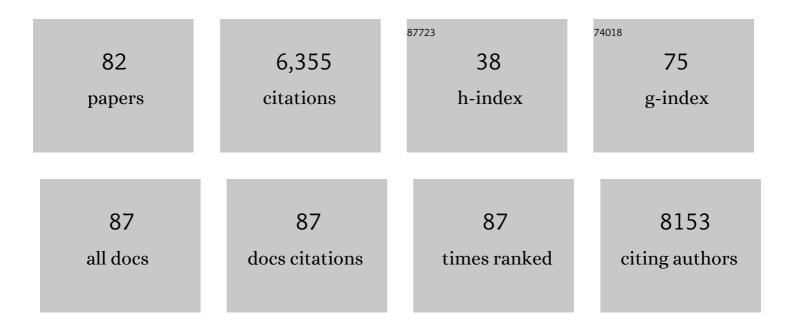
Brian J Kirby

List of Publications by Year in descending order

Source: https://exaly.com/author-pdf/5974928/publications.pdf Version: 2024-02-01



RDIAN L KIDRY

#	Article	IF	CITATIONS
1	Acquired chemoresistance drives spatial heterogeneity, chemoprotection and collective migration in pancreatic tumor spheroids. PLoS ONE, 2022, 17, e0267882.	1.1	0
2	Rational design protocols for size-based particle sorting microdevices using symmetry-induced cyclical dynamics. Physical Review E, 2020, 101, 032125.	0.8	1
3	Microfluidic chip for label-free removal of teratoma-forming cells from therapeutic human stem cells. Journal of Immunology and Regenerative Medicine, 2020, 10, 100030.	0.2	2
4	Three-Dimensional Numerical Modeling of Surface-Acoustic-Wave Devices: Acoustophoresis of Micro- and Nanoparticles Including Streaming. Physical Review Applied, 2019, 12, .	1.5	39
5	Using Acoustic Perturbations to Dynamically Tune Shear Thickening in Colloidal Suspensions. Physical Review Letters, 2019, 123, 128001.	2.9	17
6	Scalable Synthesis of Switchable Assemblies of Gold Nanorod Lyotropic Liquid Crystal Nanocomposites. Small, 2019, 15, 1901666.	5.2	12
7	anti-EGFR capture mitigates EMT- and chemoresistance-associated heterogeneity in a resistance-profiling CTC platform. Analytical Biochemistry, 2019, 577, 26-33.	1.1	12
8	Charge Scaling Manifesto: A Way of Reconciling the Inherently Macroscopic and Microscopic Natures of Molecular Simulations. Journal of Physical Chemistry Letters, 2019, 10, 7531-7536.	2.1	83
9	Expression of AR-V7 and ARv567es in Circulating Tumor Cells Correlates with Outcomes to Taxane Therapy in Men with Metastatic Prostate Cancer Treated in TAXYNERGY. Clinical Cancer Research, 2019, 25, 1880-1888.	3.2	92
10	How Biophysical Forces Regulate Human B Cell Lymphomas. Cell Reports, 2018, 23, 499-511.	2.9	30
11	Decorrelation correction for nanoparticle tracking analysis of dilute polydisperse suspensions in bulk flow. Physical Review E, 2017, 95, 033305.	0.8	4
12	Separation of 300 and 100 nm Particles in Fabry–Perot Acoustofluidic Resonators. Analytical Chemistry, 2017, 89, 12192-12200.	3.2	53
13	Randomized, Noncomparative, Phase II Trial of Early Switch From Docetaxel to Cabazitaxel or Vice Versa, With Integrated Biomarker Analysis, in Men With Chemotherapy-NaÃ⁻ve, Metastatic, Castration-Resistant Prostate Cancer. Journal of Clinical Oncology, 2017, 35, 3181-3188.	0.8	73
14	Surface conductivity in electrokinetic systems with porous and charged interfaces: Analytical approximations and numerical results. Electrophoresis, 2016, 37, 1979-1991.	1.3	4
15	Automated electrorotation shows electrokinetic separation of pancreatic cancer cells is robust to acquired chemotherapy resistance, serum starvation, and EMT. Biomicrofluidics, 2016, 10, 064109.	1.2	30
16	Comparison and optimization of machine learning methods for automated classification of circulating tumor cells. Cytometry Part A: the Journal of the International Society for Analytical Cytology, 2016, 89, 922-931.	1.1	27
17	2563 Screening and baseline analysis of circulating tumor cell (CTC) counts and androgen receptor (AR) localization with clinical characteristics of men with metastatic castration-resistant prostate cancer (mCRPC) in TAXYNERGY. European Journal of Cancer, 2015, 51, S498-S499.	1.3	0
18	A transfer function approach for predicting rare cell capture microdevice performance. Biomedical Microdevices, 2015, 17, 9956.	1.4	2

#	Article	IF	CITATIONS
19	Enhancing sensitivity and specificity in rare cell capture microdevices with dielectrophoresis. Biomicrofluidics, 2015, 9, 014116.	1.2	19
20	Measurement of Lipid Accumulation in Chlorella vulgaris via Flow Cytometry and Liquid-State ¹H NMR Spectroscopy for Development of an NMR-Traceable Flow Cytometry Protocol. PLoS ONE, 2015, 10, e0134846.	1.1	15
21	Baseline analysis of circulating tumor cell (CTC) enumeration and androgen receptor (AR) localization in men with metastatic castration-resistant prostate cancer (mCRPC) in TAXYNERGY Journal of Clinical Oncology, 2015, 33, 5031-5031.	0.8	1
22	Microfluidic isolation of cancer-cell-derived microvesicles from hetergeneous extracellular shed vesicle populations. Biomedical Microdevices, 2014, 16, 869-877.	1.4	87
23	Single-Cell Copy Number Analysis of Prostate Cancer Cells Captured with Geometrically Enhanced Differential Immunocapture Microdevices. Analytical Chemistry, 2014, 86, 11013-11017.	3.2	11
24	Characterization of microfluidic shear-dependent epithelial cell adhesion molecule immunocapture and enrichment of pancreatic cancer cells from blood cells with dielectrophoresis. Biomicrofluidics, 2014, 8, 044107.	1.2	23
25	Cancerous epithelial cell lines shed extracellular vesicles with a bimodal size distribution that is sensitive to glutamine inhibition. Physical Biology, 2014, 11, 065001.	0.8	21
26	Microfluidic immunocapture of circulating pancreatic cells using parallel EpCAM and MUC1 capture: characterization, optimization and downstream analysis. Lab on A Chip, 2014, 14, 1775-1784.	3.1	107
27	Parametric control of collision rates and capture rates in geometrically enhanced differential immunocapture (GEDI) microfluidic devices for rare cell capture. Biomedical Microdevices, 2014, 16, 143-151.	1.4	24
28	Circulating Tumor Cells in Prostate Cancer Diagnosis and Monitoring: An Appraisal of Clinical Potential. Molecular Diagnosis and Therapy, 2014, 18, 389-402.	1.6	51
29	Isolation of breast cancer and gastric cancer circulating tumor cells by use of an anti HER2-based microfluidic device. Lab on A Chip, 2014, 14, 147-156.	3.1	94
30	Electrokinetic Measurements of Thin Nafion Films. Langmuir, 2014, 30, 1985-1993.	1.6	13
31	Detection of Circulating Pancreas Epithelial Cells in Patients With Pancreatic Cystic Lesions. Gastroenterology, 2014, 146, 647-651.	0.6	191
32	Detection of algal lipid accumulation due to nitrogen limitation via dielectric spectroscopy of Chlamydomonas reinhardtii suspensions in a coaxial transmission line sample cell. Bioresource Technology, 2013, 143, 623-631.	4.8	33
33	Culture of primary rat hippocampal neurons: design, analysis, and optimization of a microfluidic device for cell seeding, coherent growth, and solute delivery. Biomedical Microdevices, 2013, 15, 97-108.	1.4	9
34	Transport and collision dynamics in periodic asymmetric obstacle arrays: Rational design of microfluidic rare-cell immunocapture devices. Physical Review E, 2013, 88, 032136.	0.8	20
35	Characterization of a hybrid dielectrophoresis and immunocapture microfluidic system for cancer cell capture. Electrophoresis, 2013, 34, 2970-2979.	1.3	14
36	Microfluidic Enrichment of Mouse Epidermal Stem Cells and Validation of Stem Cell Proliferation In Vitro. Tissue Engineering - Part C: Methods, 2013, 19, 765-773.	1.1	15

#	Article	IF	CITATIONS
37	Enrichment of prostate cancer cells from blood cells with a hybrid dielectrophoresis and immunocapture microfluidic system. Biomedical Microdevices, 2013, 15, 941-948.	1.4	49
38	Force and flux relations for flows of ionic solutions between parallel plates with porous and charged layers. Physical Review E, 2013, 88, 042408.	0.8	3
39	TAXYNERGY (NCT01718353): A randomized phase II trial examining an early switch from first-line docetaxel to cabazitaxel, or cabazitaxel to docetaxel, in men with metastatic castration-resistant prostate cancer (mCRPC) Journal of Clinical Oncology, 2013, 31, TPS5100-TPS5100.	0.8	4
40	Microfluidic transport in microdevices for rare cell capture. Electrophoresis, 2012, 33, 3133-3142.	1.3	38
41	Soft diffuse interfaces in electrokinetics – theory and experiment for transport in charged diffuse layers. Soft Matter, 2012, 8, 10598.	1.2	60
42	Isolation and characterization of circulating tumor cells in prostate cancer. Frontiers in Oncology, 2012, 2, 131.	1.3	38
43	Functional Characterization of Circulating Tumor Cells with a Prostate-Cancer-Specific Microfluidic Device. PLoS ONE, 2012, 7, e35976.	1.1	185
44	Immunocapture of prostate cancer cells by use of anti-PSMA antibodies in microdevices. Biomedical Microdevices, 2012, 14, 401-407.	1.4	42
45	Micro-total analysis system for virus detection: microfluidic pre-concentration coupled to liposome-based detection. Analytical and Bioanalytical Chemistry, 2012, 402, 315-323.	1.9	59
46	Automated Dielectrophoretic Characterization of Mycobacterium smegmatis. Analytical Chemistry, 2011, 83, 3507-3515.	3.2	46
47	Methods for Photocrosslinking Alginate Hydrogel Scaffolds with High Cell Viability. Tissue Engineering - Part C: Methods, 2011, 17, 173-179.	1.1	167
48	Integrated microfluidic preconcentrator and immunobiosensor. Microfluidics and Nanofluidics, 2011, 11, 537-544.	1.0	10
49	Stiffness of photocrosslinked RGDâ€alginate gels regulates adipose progenitor cell behavior. Biotechnology and Bioengineering, 2011, 108, 1683-1692.	1.7	91
50	Rare cell capture in microfluidic devices. Chemical Engineering Science, 2011, 66, 1508-1522.	1.9	171
51	Ambient pressure effects on the electrokinetic potential of Zeonor–water interfaces. Journal of Colloid and Interface Science, 2011, 361, 381-387.	5.0	3
52	Electrothermal flow effects in insulating (electrodeless) dielectrophoresis systems. Electrophoresis, 2010, 31, 3622-3633.	1.3	88
53	Capture of circulating tumor cells from whole blood of prostate cancer patients using geometrically enhanced differential immunocapture (GEDI) and a prostate-specific antibody. Lab on A Chip, 2010, 10, 27-29.	3.1	346
54	Control of the Electromechanical Properties of Alginate Hydrogels via Ionic and Covalent Cross-Linking and Microparticle Doping. Biomacromolecules, 2010, 11, 2184-2189.	2.6	8

#	Article	IF	CITATIONS
55	Transient ζâ€potential measurements in hydrophobic, TOPAS microfluidic substrates. Electrophoresis, 2009, 30, 2656-2667.	1.3	18
56	Refolding of Î ² -galactosidase: microfluidic device for reagent metering and mixing and quantification of refolding yield. Microfluidics and Nanofluidics, 2009, 7, 275-281.	1.0	8
57	Zeta potential and electroosmotic mobility in microfluidic devices fabricated from hydrophobic polymers: 1. The origins of charge. Electrophoresis, 2008, 29, 1092-1101.	1.3	170
58	Zeta potential and electroosmotic mobility in microfluidic devices fabricated from hydrophobic polymers: 2. Slip and interfacial water structure. Electrophoresis, 2008, 29, 1102-1114.	1.3	84
59	Microfluidic devices for terahertz spectroscopy of biomolecules. Optics Express, 2008, 16, 1577.	1.7	110
60	Continuous-Flow Particle Separation by 3D Insulative Dielectrophoresis Using Coherently Shaped, dc-Biased, ac Electric Fields. Analytical Chemistry, 2007, 79, 7291-7300.	3.2	154
61	Low-Light-Level Optical Interactions with Rubidium Vapor in a Photonic Band-Gap Fiber. Physical Review Letters, 2006, 97, 023603.	2.9	173
62	Inorganic Proton Exchange Membranes. , 2006, , 1135.		0
63	Nonlinear optical interactions with Rubidium atoms confined in a hollow-core photonic crystal fiber. , 2006, , .		1
64	The zeta potential of cyclo-olefin polymer microchannels and its effects on insulative (electrodeless) dielectrophoresis particle trapping devices. Electrophoresis, 2005, 26, 1792-1799.	1.3	93
65	Microfluidic routing of aqueous and organic flows at high pressures: fabrication and characterization of integrated polymer microvalve elements. Lab on A Chip, 2005, 5, 184.	3.1	27
66	Microchip HPLC of Peptides and Proteins. Analytical Chemistry, 2005, 77, 2997-3000.	3.2	88
67	Zeta potential of microfluidic substrates: 1. Theory, experimental techniques, and effects on separations. Electrophoresis, 2004, 25, 187-202.	1.3	834
68	Zeta potential of microfluidic substrates: 2. Data for polymers. Electrophoresis, 2004, 25, 203-213.	1.3	403
69	Electrophoretic Concentration of Proteins at Laser-Patterned Nanoporous Membranes in Microchips. Analytical Chemistry, 2004, 76, 4589-4592.	3.2	154
70	Microchip Dialysis of Proteins Using in Situ Photopatterned Nanoporous Polymer Membranes. Analytical Chemistry, 2004, 76, 2367-2373.	3.2	107
71	On-Chip High-Pressure Picoliter Injector for Pressure-Driven Flow through Porous Media. Analytical Chemistry, 2004, 76, 5063-5068.	3.2	53
72	Effects of ammonioalkyl sulfonate internal salts on electrokinetic micropump performance and reversed-phase high-performance liquid chromatographic separations. Journal of Chromatography A, 2003, 1013, 93-101.	1.8	18

#	Article	IF	CITATIONS
73	Increasing the performance of high-pressure, high-efficiency electrokinetic micropumps using zwitterionic solute additives. Sensors and Actuators B: Chemical, 2003, 92, 37-43.	4.0	60
74	Programmable modification of cell adhesion and zeta potential in silica microchips. Lab on A Chip, 2003, 3, 5.	3.1	79
75	Miniature and Microchip Technologies. Journal of Chromatography Library, 2003, , 659-685.	0.1	4
76	Linear excitation schemes for IR planar-induced fluorescence imaging of CO and CO_2. Applied Optics, 2002, 41, 1190.	2.1	31
77	Voltage-addressable on/off microvalves for high-pressure microchip separations. Journal of Chromatography A, 2002, 979, 147-154.	1.8	56
78	CO_2 imaging with saturated planar laser-induced vibrational fluorescence. Applied Optics, 2001, 40, 6136.	2.1	20
79	Imaging of CO and CO2 using infrared planar laser-induced fluorescence. Proceedings of the Combustion Institute, 2000, 28, 253-259.	2.4	32
80	Planar laser-induced fluorescence imaging of carbon monoxide using vibrational (infrared) transitions. Applied Physics B: Lasers and Optics, 1999, 69, 505-507.	1.1	49
81	Measurements and modeling of acetone laser-induced fluorescence with implications for temperature-imaging diagnostics. Applied Optics, 1998, 37, 4963.	2.1	228
82	Effects of heater surface orientation on the critical heat flux—I. An experimental evaluation of models for subcooled pool boiling. International Journal of Heat and Mass Transfer, 1997, 40, 4007-4019.	2.5	50